Austrian Journal of Earth Sciences | Volume 98 | 68 - 76 | Vienna | 2005

Organic maturation within the Central Northern Calcareous Alps (Eastern Alps)

Gerd RANTITSCH[1)] & Barbara RUSSEGGER[2)]

KEYWORDS

very low-grade metamorphism
Northern Calcareous Alps
vitrinite reflectance
thermal modeling
Jurassic orogeny
Eastern Alps

[1)] Department of Applied Geosciences and Geophysics, Montanuniversität Leoben, Austria, A-8700 Leoben, Austria, Email: gerd.rantitsch@mu-leoben.at

[2)] Library of the University of Graz, A-8010 Graz, Austria

Abstract

Organic maturation within the central Northern Calcareous Alps (Eastern Alps) has been investigated using vitrinite reflectance data from Upper Permian to Upper Cretaceous strata of the Stauffen-Höllengebirge Nappe, Dachstein Nappe, Tennengebirge Block and Lammer Unit. Within the Lammer Unit a metamorphic break is observed between the Strubberg Formation and the tectonically overlying Schwarzenberg Complex and Losegg-Hofpürgl slice. Vitrinite reflectance within the Dachstein Nappe and the Stauffen-Höllengebirge Nappe resembles the values within the Schwarzenberg Complex. The thermal overprint of the Tennengebirge Block and the Strubberg Formation is explained by metamorphism due to Late Jurassic imbrication of fault-bounded blocks. A numerical heat flow model explains the thermal overprint of the Dachstein Nappe by sedimentary burial during Mesozoic to Cenozoic times.

Im Zentralteil der Nördlichen Kalkalpen wurde der Grad der organischen Metamorphose durch die Messung der Vitrinitreflexion in oberpermischen bis oberkretazischen Sedimenten der Stauffen-Höllengebirge Decke, der Dachstein Decke, des Tennengebirge Blocks und der Lammer Einheit erfasst. Der tektonische Kontakt zwischen der Lammer Einheit und den tektonisch aufliegenden Komplexen des Schwarzenbergs und der Losegg-Hofpürgl Schuppe ist durch einen Metamorphosesprung gekennzeichnet. Die Vitrinitreflexion innerhalb der Dachstein- und Stauffen-Höllengebirge Decke entspricht den Werten innerhalb des Schwarzenberg Komplexes. Die thermische Überprägung des Tennengebirge Blocks und der Strubberg Formation wird durch die metamorphe Überprägung während der spätjurassischen Imbrikation von störungsbegrenzten Blöcken erklärt. Ein numerisches Wärmeflussmodell erklärt die thermische Überprägung der Dachstein Decke durch die mesozoische bis känozoische sedimentäre Auflast der Schichtfolge.

1. Introduction

The Northern Calcareous Alps (NCA) are an elongated fold-and-thrust-belt (Linzer et al. 1995) within the Eastern Alps (Fig. 1). The classical tectonic subdivision describes a lower Bavaric, an intermediate Tirolic and an upper Juvavic nappe group (Tollmann, 1976; Mandl, 2000). Whereas the Bavaric and the Tirolic units involve sediments of a Triassic to Jurassic carbonate platform facing the western Tethyan Ocean, the Juvavic units derived from the platform rim and outer shelf area (Hallstatt Zone). Based on stratigraphic, structural, metamorphic and geochronological data from the central NCA, Frisch and Gawlick (2003) proposed an alternative nappe concept in which the Juvavic Dachstein Nappe is a subunit of the Tirolic nappe group and deeper shelf sediments of the former Hallstatt Zone are parts of a flysch succession (Hallstatt mélange).

Because the thermal structure of fold-and–thrust-belts is usually attributed to thrust-related processes like burial by thrust sheets or shear heating along thrust zones (e.g. Warr et al., 1996), detailed metamorphic studies can contribute significantly to controversies about opposing nappe concepts. It was demonstrated in numerous studies that the use of organic metamorphic parameters resulted in the construction of the most detailed and meaningful metamorphic maps. Moreover, the sensitive and irreversible response of organic matter to subtle temperature variations and the well-known kinetics of organic maturation allow the calibration of thermal models which give a closer insight to thermal processes in higher crustal levels. However, the central segment of the NCA, the key area of the still ongoing debate about the internal structure of the NCA (Tollmann, 1976 vs. Neubauer, 1994 and Schweigl and Neubauer, 1997 vs. Frisch and Gawlick, 2003), is only sparsely covered by organic maturity data. In this contribution, we present therefore vitrinite reflectance data to complete the pattern of organic metamorphism and to give an insight in the thermal structure of this section.

2. Geological setting

The Late Triassic facial distribution of the NCA describes a carbonate platform (Dachstein platform) faced in the south by the outer shelf and shelf edge realm of the Hallstatt Zone (Haas et al., 1995, Gawlick et al., 1999; Mandl, 2000). This facies belt was destroyed during the Late Jurassic closure of the adjacent Meliata Ocean (Neubauer, 1994; Neubauer et al., 2000; Mandl, 2000; Frisch and Gawlick, 2003). Late Jurassic to Eocene thrusting (Mandl, 2000; Frisch and Gawlick, 2003) and Early to Middle Miocene block fragmentation (Linzer et al., 1995; Frisch et al., 1998; Frisch and Gawlick, 2003) determined the present tectonic structure of the NCA.

In the traditional model (Tollmann, 1976; Mandl, 2000), Late Jurassic to Cretaceous north-directed thrusting displaced the deeper shelf and platform sediments of the Hallstatt Zone as a

Juvavic Nappe Complex (involving the Dachstein Nappe, Fig. 2) upon the Tirolic Nappe Complex (involving the Stauffen-Höllengebirge Nappe, Fig. 2). Jurassic basins of the Tirolic Nappe Complex containing gravity transported slices (olistoliths) of the Hallstatt Zone were overthrusted by the Juvavic Nappe Complex.

The contrary model by Frisch and Gawlick (2003) describes a Callovian to Oxfordian accretionary wedge which was completely destroyed during the Late Jurassic. The debris of this wedge was transported towards the north into a radiolaritic flysch basin (Lammer Basin) which subsided on top of the Dachstein carbonate platform. Progressive north-directed thrusting separated the Dachstein carbonate platform into a lower- and an upper-Tirolic nappe. The Stauffen-Höllengebirge Nappe is interpreted as a segment of the lower-Tirolic Nappe whereas the Dachstein Nappe is interpreted as a segment of the upper-Tirolic Nappe. During Oxfordian to Tithonian times radiolaritic basins developed at the frontal ramp of the upper Tirolic nappe (Tauglboden Basin) and out-of-sequence upon the Lammer Basin (Sillenkopf Basin). During the Eocene period, out-of-sequence thrusting transported the Dachstein Nappe upon sediments of the Hallstatt Zone (Frisch and Gawlick, 2003).

In the western and central part of the NCA there is a general north to south and east to west increase in the metamorphic overprint (Kralik et al., 1987; Krumm et al., 1988; Petschick, 1989; Kürmann, 1993; Ferreiro Mählmann, 1994). In this segment, Petschick (1989) and Ferreiro Mählmann and Petschick (1995) proposed a (pre-tectonic) Permian to Early Cretaceous diastathermal metamorphism with burial temperatures up to 300° C, a syn-tectonic thermal event during Early Cretaceous to Turonian times with burial temperatures of c. 250° C, and a posttectonic thermal event acting in the Early Cenozoic period. In the northeastern part of the NCA an eastward increase in the thermal overprint is indicated by sub-bituminous to high-volatile bituminous Carnian (Lunz) coals, implying maximum burial temperatures of c. 170° C (Sachsenhofer, 1987).

According to Frisch and Gawlick (2003) the Late Jurassic imbrication of the accretionary wedge metamorphosed the olistoliths of the Hallstatt Zone. Conodont Alteration Indices (ranging from CAI 1.0 to CAI 7.0) within carbonate olistoliths of the Hallstatt Zone (Gawlick and Königshof, 1993; Gawlick et al., 1994; Gawlick and Höpfer, 1996) support this model. According to data from the entire NCA, Spötl and Hasenhüttl (1998) concluded that the imbrication is responsible for the variation of vitrinite reflectance and illite crystallinity in the Upper Permian Haselgebirge. From calcite-dolomite thermometry Gawlick and Höpfer (1996) supposed maximum burial temperatures of 350° C to 490° C at minimum pressures of 6-8 kbar during this event. A large segment of the wedge (Tennengebirge block of the Ultra-Tirolic nappe sensu Frisch and Gawlick, 2003) was deeply buried and metamorphosed (Frisch and Gawlick, 2003). Kralik and Schramm (1994) explained the lower thermal overprint in the western segment of the Stauffen-Höllengebirge Nappe by a younger metamorphic event which was induced by thrusting combined with fluid circulation. Geochronological data constrain the age of metamorphism between 130 and 140 Ma (Kralik et al., 1987; Kralik and Schramm, 1994).

Progressive thrusting was followed by a phase of uplift and erosion during the Early Cretaceous before the Gosau basins (Figs. 1, 2) subsided during Turonian to Eocene times on top of the nappe stack (Wagreich and Faupl, 1994; Wagreich, 1995, 2001; Wagreich and Decker, 2001).

The Lammer Unit (Tollmann, 1976; Fig. 2) is the key area for the evaluation of the Late Jurassic tectonometamorphic history. At the southern margin of this unit, 250 m thick Upper Jurassic radiolaritic flysch sediments (Strubberg Formation) were deposited within the Lammer Basin (Gawlick et al., 1999), which

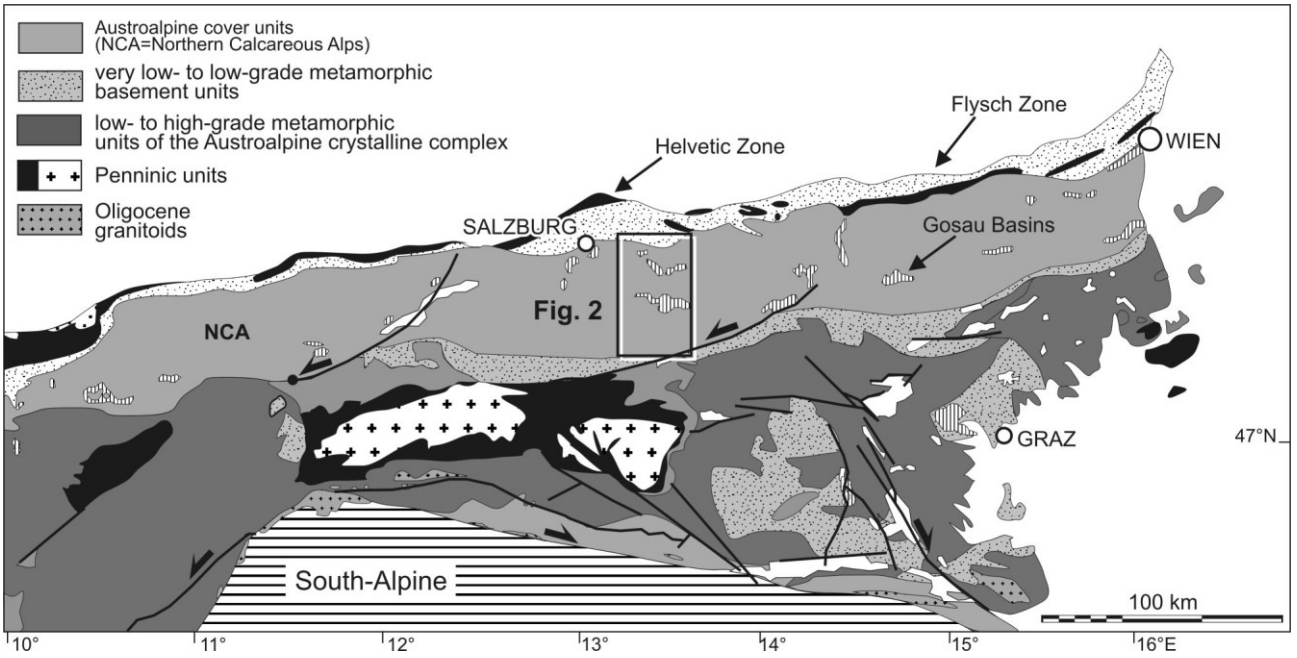

Figure 1: Location of the study area within the Alps.

itself is a part of the upper-Tirolic unit of Frisch and Gawlick (2003). These sediments are tectonically (Gawlick et al., 1990; Schweigl and Neubauer, 1997) separated towards the north from more than 1000 m thick Scythian to Liassic strata of the Schwarzenberg Complex (Tollmann, 1976; Gawlick et al., 1990; Gawlick, 1996; Frisch and Gawlick, 2003). According to Gawlick et al. (1990) the Schwarzenberg Complex is an olistolith which slided gravitationally into Upper Jurassic flysch sediments of the Lammer Basin. Other authors postulated a classical Juvavic position of the Schwarzenberg Unit (Tollmann, 1976; Plöchinger, 1980; Schweigl and Neubauer, 1997; Mandl, 2000).

3. Samples and methods

Organic maturity was determined in samples from the Scythian Werfen Formation, from the Carnian Raibl Formation, from the Upper Jurassic Strubberg Formation and from Upper Cretaceous Gosau sediments. Random vitrinite reflectance values were measured on sections polished perpendicular to the foliation under oil immersion in non-polarized light at a wavelength of 546 nm. Some samples were characterized by the apparent maximum and minimum vitrinite reflectance values measured in polarized light. The data base (Tab. 1) is completed by published vitrinite reflectance data from the Upper Permian Haselgebirge (Spötl and Hasenhüttl, 1998), by vitrinite reflectance data from Carnian strata of the Grünau I well (Colins et al., 1992), by vitrinite reflectance data from the Upper Jurassic Strubberg Formation (Rantitsch et al., 2003), and by unpublished vitrinite reflectance values from Gosau sediments (Sachsenhofer, unpublished).

Petromod 9.0 1D software of IES, Jülich was used to model paleo-heat flow during burial heating of the NCA. Input data include the thickness of stratigraphic units, the physical properties of their lithologies, the temperature at the sediment–water interface, information on the stratigraphy and lithology of the modelled section, and the temporal evolution of the heat flow at the base of the sedimentary succession. This information was used to reconstruct decompacted subsidence histories and the temperature field through time, calibrated by observed vitrinite reflectance values. For the calculation of vitrinite reflectance, the kinetic EASY%Ro method of Sweeney and Burnham (1990) was applied. Temperature and time are considered the prime factors controlling vitrinite maturation. In the used algorithm heat enters at the base of the decompacted stratigraphic succession and is transferred conductively according to temperature gradients. Only forced (i.e. compaction induced) convection is directly taken into account. Effects of free convective fluid flow systems were not simulated. Effects of thrusting within the succession were also not taken into account.

4. Vitrinite reflectance data

Vitrinite reflectance values from the Upper Jurassic Strubberg Formation range between 2.0 and 3.8 %Ro (Rantitsch et al., 2003). Significantly lower values (0.8 to 1.1 %Ro) were measured in samples from the Carnian Raibl Formation of the Dachstein and Stauffen-Höllengebirge Nappe (Tab. 1, Fig. 2).

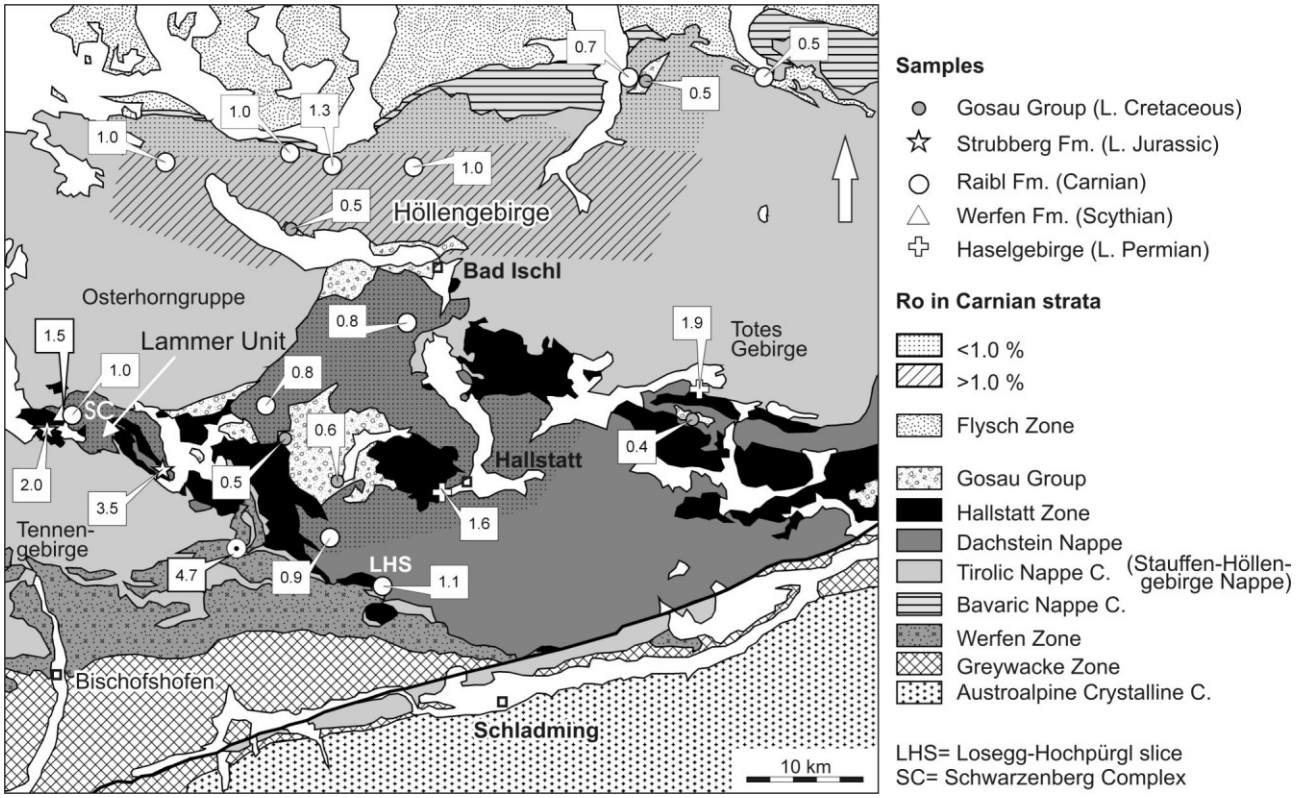

Figure 2: Vitrinite reflectance (%Ro) within the central Northern Calcareous Alps (basemap redrawn from Mandl, 2000). The data give an average from all samples of one sample locality (Tab. 1). One sample locality within the Tennengebirge Range (circle symbol with a central point) is characterized by a %Rmax value as a mean value of two samples (Tab. 1).

Although the sample grid does not cover the southern segments of the nappes, mapped CAI (Gawlick et al., 1994) and illite crystallinity (Kralik et al., 1987; Kralik and Schramm, 1994) values suggest similar vitrinite reflectance values in the uncovered regions. Carnian samples from the Losegg-Hofpürgl slice (Fig. 2) and from the Schwarzenberg Complex (Fig. 2) show a vitrinite reflectance of 1.1 and 1.0 %Ro, respectively. One sample from the Scythian Werfen Formation of the Schwarzenberg Complex is characterized by 1.5 %Ro. The samples within the Tennengebirge Range show a high vitrinite reflectance of 4.7 %Rmax (mean of two samples, see Tab. 1, Fig. 2). Upper Cretaceous Gosau sediments are characterized by a vitrinite reflectance of 0.5 to 0.6 %Rmax (Fig. 2). Samples from two gypsum-anhydrite mines (Fig. 2) indicate a mean vitrinite reflectance of 1.9 to 2.0 %Ro in the Upper Permian Haselgebirge (Spötl and Hasenhüttl, 1998).

Sample	Formation	Tectonic Unit	Locality	X	Y	Ro	s	Rmax	s	Rmin	s	N
S2	Hochmoos Fm	Gosau Basin	Gosauschmidt	463780	268630	0.56	0.26					8
34	Grabenbach Fm	Gosau Basin	Rußbach	459950	273840	0.54	0.11					38
S	Coniac-Santon Coal	Gosau Basin	Aschau/Strobl	461950	288700	0.47	0.02					
S	Coniac-Santon Coal	Gosau Basin	Mondsee			0.49	0.03					
S	Turonian-Santonian Coal	Gosau Basin	Weißenbachalm			0.43						
1	Raibel Fm	Dachstein Nappe	Gosaukamm	460730	267820	0.89	0.18					11
4	Raibel Fm	Dachstein Nappe	Gosaukamm	461960	266310	0.86	0.09					12
5	Raibel Fm	Dachstein Nappe	Gosaukamm	462000	266410	0.98	0.12					39
9	Raibel Fm	Höllengebirge Nappe	Mondsee	458160	295390	1.06	1.06					3
10B	Raibel Fm	Höllengebirge Nappe	Mondsee	457900	295840	0.95	0.31					23
11	Raibel Fm	Höllengebirge Nappe	Mondsee	457050	296000	0.96	0.22					31
13	Raibel Fm	Höllengebirge Nappe	Pöllach	450550	294240	0.95	0.18					14
20A	Raibel Fm	Höllengebirge Nappe	Weißenbach	468630	294730	0.99	0.12					8
20B	Raibel Fm	Höllengebirge Nappe	Weißenbach	468630	294730	1.01	0.14					28
21	Raibel Fm	Höllengebirge Nappe	Attersee	462740	294460	1.27	0.23					6
22	Raibel Fm	Höllengebirge Nappe	Traunsee	485910	301560	0.66	0.11					30
24	Raibel Fm	Schwarzenberg Complex	Wallingalm	444480	273970	1.03	0.14					17
25	Raibel Fm	Losegg-Hofpürgl slice	Hofpürglhütte	464020	261120	0.84	0.14					6
26	Raibel Fm	Losegg-Hofpürgl slice	Hofpürglhütte	463920	261090	1.13	0.14					24
27	Raibel Fm	Losegg-Hofpürgl slice	Hofpürglhütte	463920	261090	1.21	0.19					29
30	Raibel Fm	Dachstein Nappe	Lauffen	469390	282560	0.83	0.18					25
31	Raibel Fm	Dachstein Nappe	Lauffen	469390	282560	0.78	0.10					31
32	Raibel Fm	Dachstein Nappe	Lauffen	469390	282560	0.72	0.10					17
33	Raibel Fm	Dachstein Nappe	Rinnbergalm	458230	276070	0.81	0.10					30
35	Raibel Fm	Tennengebirge Range	Krailberg	455260	263770			5.33	1.37	2.25	0.65	26
36	Raibel Fm	Tennengebirge Range	Krailberg	455410	264180			4.09	1.36	1.63	0.43	17
Co	Reifling Fm	Höllengebirge Nappe	Grünau I			0.50						
3	Reifling Fm	Dachstein Nappe	Gosaukamm	461810	266310	0.69	0.16					28
R	Strubberg Fm	Lammer Unit	Strubberg	448490	268380	3.20	0.10					50
R	Strubberg Fm	Lammer Unit	Strubberg	448490	268380	3.73	0.26					17
R	Strubberg Fm	Lammer Unit	Strubberg	448490	268380	3.83	0.20					50
7	Strubberg Fm	Lammer Unit	Strubberg	448240	269010			4.12	0.45	2.78	0.65	12
R	Strubberg Fm	Lammer Unit	Strubberg	448490	268380	3.20	0.10					50
R	Strubberg Fm	Lammer Unit	Strubberg	448490	268380	3.73	0.26					17
R	Strubberg Fm	Lammer Unit	Strubberg	448490	268380	3.83	0.20					50
7	Strubberg Fm	Lammer Unit	Strubberg	448240	269010			4.12	0.45	2.78	0.65	12
8	Strubberg Fm	Lammer Unit	Strubberg	448240	269010			4.16	0.24	2.47	0.67	11
S1	Strubberg Fm	Lammer Unit	Lammeregg	441000	271230	2.06	0.06					7
R	Strubberg Fm	Lammer Unit	Lammeregg	441000	271230	1.87	0.12					50
R	Strubberg Fm	Lammer Unit	Lammeregg	441000	271230	1.98	0.12					50
R	Strubberg Fm	Lammer Unit	Lammeregg	441000	271230	1.97	0.13					13
R	Strubberg Fm	Lammer Unit	Lammeregg	441000	271230	1.98	0.09					50
S4	Strubberg Fm	Lammer Unit	Lammeregg	441000	271230	2.06	0.20					26
23	Werfen Fm	Lammer Unit	Wallingalm	444280	273810	1.48	0.24					7
Sp	Haselgebirge	Hallstatt Unit	Hallstatt			1.63	0.10					202
Sp	Haselgebirge	Hallstatt Unit	Grundlsee			1.90	0.20					81

Table 1: Mean random (Ro), maximum (Rmax) and minimum (Rmin) vitrinite reflectance within the central Calcareous Alps (s= standard deviation, N= number of measurements). Samples S are unpublished values of R. Sachsenhofer. Sample Co is derived from Colins et al. (1992), samples Sp from Spötl and Hasenhüttl (1998), and samples R from Rantitsch et al. (2003). The coordinates (X, Y) refer to the Austrian M31 coordinate system.

5. Discussion

5.1 Heating of the Tennengebirge block and Strubberg formation

Vitrinite reflectance values from the Strubberg Formation range between 2.0 and 3.8 %Ro (Tab. 1). Based on the time-independent temperature regression of Barker (1988) these values correspond to paleotemperatures of 220° C to 290° C. In contrast, Carnian samples from the Losegg-Hofpürgl slice (an olistolith at the southeastern margin of the Lammer Unit, Tollmann, 1976, Fig. 2) and from the Schwarzenberg Complex show a vitrinite reflectance of 1.1 and 1.0 %Ro. These values correspond roughly to CAI values of this region which describe a top-to-bottom increase of CAI 1.0 to CAI 2.5 (Gawlick, 1997). Gawlick (1997) correlated them with maximum burial temperatures below 180° C.

To evaluate the thermal history it is important to note that the model of Frisch and Gawlick (2003) expects a burial heating pattern (i.e. an increase of the metamorphic rank with increasing burial depths) within the Lammer Basin (Gawlick, 1997). In a consistent model, the Lammer Basin is composed of olistoliths (involving the Schwarzenberg Complex) floating in an unmetamorphosed sedimentary matrix (Strubberg Formation). However, the Strubberg Formation is tectonically separated from the overlying Schwarzenberg Complex (Gawlick et al, 1990; Gawlick and Frisch, 2003). This fact and the observation of significantly contrasting vitrinite reflectance values in these units argue against the supposition of Frisch and Gawlick (2003). In our concept, the high thermal overprint of the Strubberg Formation must be explained by a deeper burial of a tectonically separated block or by the loading of a pile of sediments on top of the exposed succession of the Strubberg Formation which was removed tectonically after the accumulation of the olistoliths of the Schwarzenberg Complex. If the latter hypothesis is correct, a more than 2000 m thick succession, composed of olistoliths floating in radiolaritic flysch sediments, filled the Lammer Basin on top of the Upper Triassic Dachstein carbonate platform, which was subsequently displaced as a Tirolic Nappe Complex sensu Frisch and Gawlick (2003). However, vitrinite reflectance values from the Carnian Raibl Formation of the Dachstein and Stauffen-Höllengebirge Nappe (subunits of the Tirolic Nappe Complex sensu Gawlick and Frisch, 2003) range between 0.8 and 1.3 %Ro and indicate

Formation	Stratigraphy	Lithology	Depositional Environment	Present Thickness [m]	Eroded Thickness [m]	Depositional Age [Ma] From	Erosion Age [Ma] To	Erosion Age [Ma] From	Erosion Age [Ma] To
Augenstein Formation	Rupelian-Aquitanian	gravel	terrestric	0	1000	34	21	21	0
Gap	Ypresian-Rupelian					52	34		
Zwieselalm Formation	Maastrichtian-Ypresian	Marls	slope	300	600	70	52	52	34
Nierental Formation	U.Campanian-Maastrichtian	Marls+Limestones	slope	400		72	70		
Ressen Formation	L.-U. Campanian	Conglomerates+Sandstones	slope	400		82	72		
Gap	L. Campanian					83	82		
Bibereck Formation	L. Campanian	Marl+Sandstone	shelf	70		84	83		
Hochmoos Formation	U. Santonian	Marl+Sandstone	shelf	250		85	84		
Grabenbach Formation	L. Santonian	Marl+Siltstones+Sandstones	shallow-marine	250		86	85		
Streiteck Formation	Coniancian	Conglomerates+Sandstones	fan-delta	80		89	86		
Kreuzgraben Formation	Turonian	Conglomerates	alluvial	300		92	89		
Gap	Valanginian-Turonian					135	92		
Schrambach Formation	Berriasian-Valanginian	Limestone		150		140	135		
Plassen Formation	Kimmeridgian-Berriasian	Limestone	platform	700		154	140		
Strubberg Formation	L. Callovian-Oxfordian	Cherts + Limestone	deep-water	250		159	154		
Klaus Formation	Aalenian-Callovian	Limestone	deep-water	10		178	159		
Adnet Formation	Hettangian-Aalenian	Limestone	deep-water	50		205	178		
Gap	Rhaetian					210	205		
Dachstein Formation	Norian	Limestone+Dolomite	platform	1200		221	210		
Raibl Formation	U. Carnian	Shale	shallow-marine	70		223	221		
Wetterstein Formation	L. Carnian	Limestone+Dolomite	platform	400		225	223		
Raming Formation	L. Carnian	Limestone	shallow-marine	300		227	225		
Hallstatt/Reifling Fm.	U. Anisian-Ladinian	Limestone	deep-water	50		236	227		
Steinalm Formation	M. Anisian	Limestone	shallow-marine	100		238	236		
Gutenstein Formation	L. Anisian	Dolomite	shallow-marine	200		242	238		
Werfen Formation	Skythian	Shale+Sandstone	shallow-marine	300		250	242		
Haselgebirge	Wuchiapingian-Skythian	Evaporites+sandstone+shale	shallow-marine	100		255	250		

Table 2: Input parameters for the 1-D thermal model compiled from Mandl (2000), Gawlick and Frisch (2002), Wagreich (1988, 1995, 2001), Wagreich and Decker (2001) and Frisch et al. (2001).

therefore a supposition of a higher metamorphic unit (Strubberg Formation) above a lower metamorphic unit. This observation contradicts the assumption of an autochthonous position of the Lammer Basin above the Dachstein carbonate platform. We suppose therefore, that Late Jurassic thrusting fragmented the Lammer Basin during the time of flysch sedimentation. As a result, the tectonically detached stratigraphic base of the basin (with the sediments of the Strubberg Formation) experienced a deeper burial than the sediments of the Dachstein and Stauffen-Höllengebirge Nappes and the tectonically overlying Schwarzenberg Complex.

Late Jurassic imbrication deeply buried the Tennengebirge Block south of the Lammer Unit (Frisch and Gawlick, 2003), an ultra-Tirolic unit according to Frisch and Gawlick (2003). Rather high vitrinite reflectance values of 4.1 to 5.3 %Rmax characterize the Carnian strata of this block (Tab. 1). These values resemble Rmax values from the Strubberg Formation (Tab. 1). Hence, the Strubberg Formation at the southern margin of the Lammer Unit shows the same metamorphic overprint as the Tennengebirge Block and therefore, may be interpreted as a part of the Tennengebirge Block (Tollmann, 1976; Gawlick et al., 1990; Schweigl and Neubauer, 1997).

Consequently, we see in the area of the central NCA evidences for a juxtaposition of tectonic blocks which are characterized by different thermal histories. Accepting the model of Frisch and Gawlick (2003) a metamorphic overprint due to Late Jurassic imbrication of fault-bounded blocks in an accretionary prism can explain the pattern of metamorphism within the Tennengebirge Block and Strubberg Formation. Radiometric age data (Kralik et al., 1987; Hejl and Grundmann, 1989) and isotopic evidences (Spötl et al., 1996, 1998) support this model.

5.2 Heating of the Dachstein and Stauffen-Höllengebirge nappe

North of the Lammer Zone, vitrinite reflectance values from the Carnian Raibl Formation of the Dachstein and Stauffen-Höllengebirge Nappe range between 0.8 and 1.3 %Ro. In both nappes the values increase slightly towards the south and suggest a break in vitrinite reflectance across the nappe boundary. Although, the incomplete spatial coverage of the sample grid does not allow a final interpretation, it is interesting to note that this observation resembles the observations of coalification breaks between individual Bavaric nappes east of the study area (Sachsenhofer, 1987).

Vitrinite reflectance within the Upper Cretaceous Gosau Basins constrains a stratigraphic trend of deceasing organic maturity within the Permian to Cretaceous sedimentary succession of the Dachstein and Stauffen-Höllengebirge nappe. This observation indicates a heating of the succession during Mesozoic to Cenozoic sedimentary burial.

5.3 Thermal modeling of the Dachstein nappe

A one-dimensional numerical model of the Dachstein Nappe reconstructs the heat flow history of the Dachstein carbonate platform which is characterized by a Late Jurassic to Early Cretaceous temperature maximum (Kralik et al., 1987; Hejl and Grundmann, 1989; Kralik and Schramm, 1994; Spötl et al., 1998). The simplified stratigraphical model includes Upper Permian evaporites (Haselgebirge), Triassic carbonate platform sediments (Wetterstein and Dachstein limestones), Lower to Upper Jurassic pelagic (Adnet, Klaus and Strubberg Formation) and Upper Jurassic carbonate platform successions (Plassen limestone), transgressively overlain by Turonian to Eocene Gosau sediments and Oligocene-Miocene fluvial gravel of the Augenstein Formation. Major subsidence events occurred during the Late Jurassic (Strubberg Formation), the Late Cretaceous (Gosau Basins) and the Oligo-/Miocene (Augenstein Formation). Thicknesses of units (Tab. 2) are based on published thickness values (Mandl, 2000; Gawlick and Frisch, 2002; Wagreich, 1988, 1995, 2001; Wagreich and Decker, 2001; Frisch et al., 2001) and do not account for tectonic reductions.

Several models were calibrated by modifying heat flow and the thickness of eroded sediments until a satisfactory fit between measured and calculated vitrinite reflectance values was obtained. In order to respect the temporal constraints, heat flow has to be raised during Late Jurassic times. Models without introduction of elevated heat flows during this time result in a Late Cretaceous temperature maximum which is not mirrored by geochronological data. If the model includes a 2000 m thick Upper Jurassic succession of olistoliths floating in radiolaritic flysch sediments (sedimentary filling of the Lammer Basin, Gawlick and Frisch, 2003) no acceptable fit between observed and calculated vitrinite reflectance values is achieved (Fig. 3). In contrast,

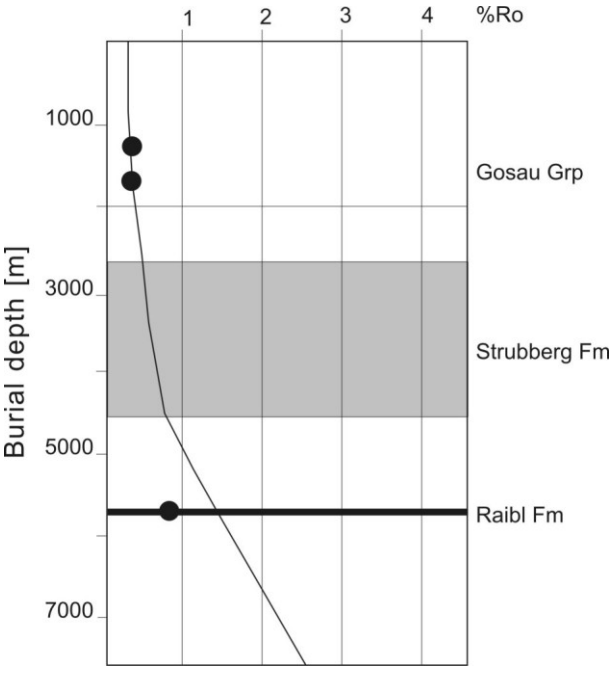

Figure 3: measured (dots) and calculated (line) vitrinite reflectance values of a thermal model characterized by a heat flow of 60 mW/m² during the Late Jurassic period. The Strubberg Formation is assumed to be 2000 m thick (Gawlick and Frisch, 2003). This scenario results in a bad calibration and therefore has to be modified. A Late Jurassic to Early Cretaceous temperature maximum cannot be modelled by the assumption of lower heat flow values.

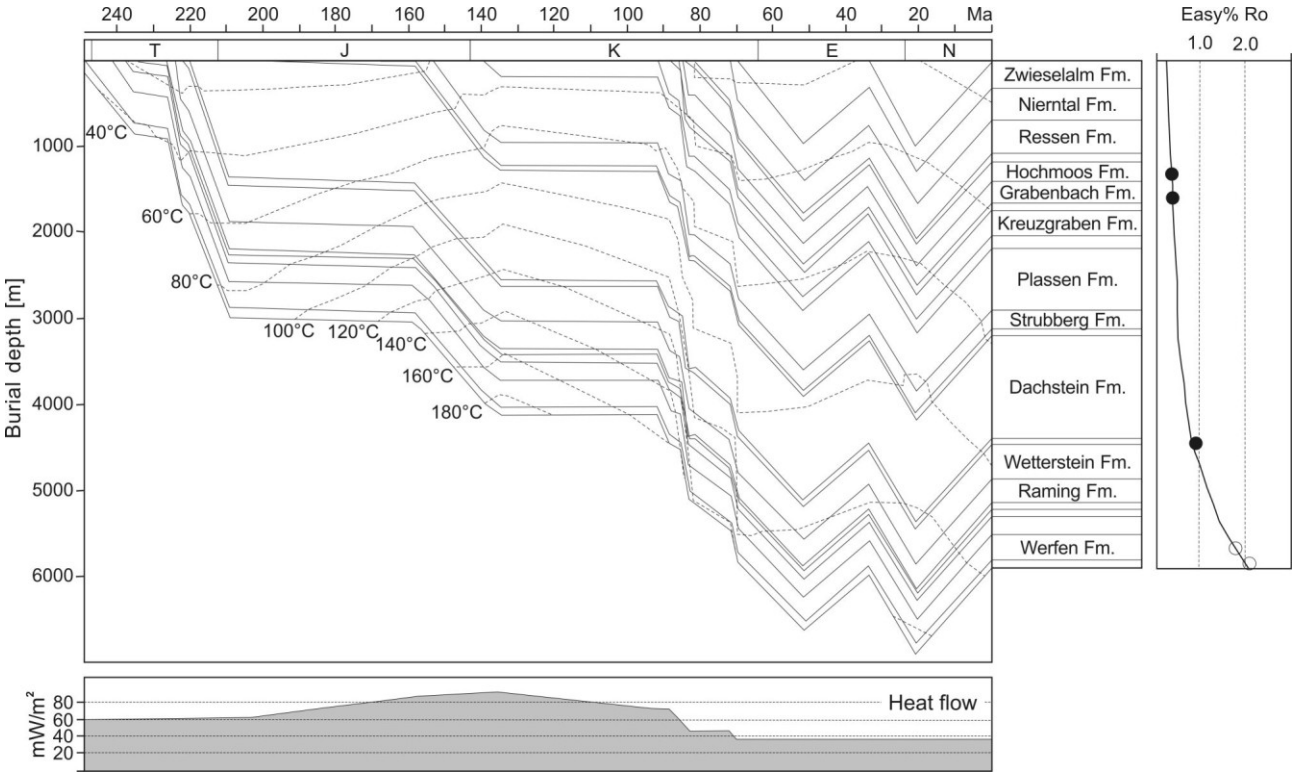

Figure 4: Burial history, temperature history and heat flow model of the Dachstein Nappe in the central Northern Calcareous Alps (for thickness data and other input parameters see Tab. 2). Dashed curves are iso-temperature lines. In the right part of the figure measured (dots representing mean vitrinite reflectance within the stratigraphic layer) and calculated vitrinite reflectance values (line) calculated on the basis of burial and temperature history using the EASY%Ro method are plotted versus depth. The model explains vitrinite reflectance values measured in the Werfen Formation of the Schwarzenberg Complex and the Upper Permian Haselgebirge from the Hallstatt Zone (open dots representing mean vitrinite reflectance within the stratigraphic layer).

a model which describes the Late Jurassic burial history of the Dachstein Nappe without incorporation of several hundred meter thick Upper Jurassic mass-flows (Tab. 2), results in a fit between observed and calculated vitrinite reflectance values (Fig. 4).

Within a narrow variability range, the model is characterized by an increasing heat flow (up to 90 mW/m²) during Jurassic times. Geologically, reasons for this increase are poorly understood. However, the Jurassic opening of the South Penninic (Piemontais-Ligurian) ocean north of the NCA may provide an explanation. Although the used algorithm does not allow the incorporation of a convective heat transfer, isotopic evidence (Kralik and Schramm, 1994; Spötl et al., 1996, 1998) demonstrates the contribution of hot circulating fluids. Therefore, the apparent increase in heat flow might have been also an effect of heat transfer by migrating fluids which influenced the temperature field. During Cretaceous times the heat flow decreased to moderate values (60 mW/m²) until the low Oligocene to recent heat flow (35 mW/m²) of an orogenic front (Sachsen-hofer, 2001) was reached.

The findings of the 1D-modeling approach demonstrate that the Mesozoic to Cenozoic burial heating by the known sedimentary column can explain the thermal overprint of the Dachstein Nappe. The thermal model fits vitrinite reflectance values which were measured within Scythian and Carnian sediments of the Schwarzenberg Complex and Losegg-Hofpürgl slice (Fig. 4). A metamorphic overprint of these blocks due to deep Late Jurassic burial in an accretionary prism is therefore highly unlikely.

6. Conclusions

Vitrinite reflectance data give information about the tectonothermal evolution of the central segment of the Northern Calcareous Alps. The following conclusions have been reached:

1. The data do not suggest an autochthonous position of the Lammer Basin on top of the Dachstein carbonate platform.
2. A break in vitrinite reflectance between the Strubberg Formation and the overlying Schwarzenberg Complex argues against a sedimentary contact of these units.
3. Metamorphism within the Tennengebirge Block and the Strubberg Formation is explained by a metamorphic overprint due to the Late Jurassic imbrication of fault-bounded blocks.
4. A numerical heat flow model explains the thermal overprint of the Dachstein carbonate platform by Mesozoic to Cenozoic burial heating with an elevated heat flow during Jurassic times.
5. Organic maturation within the Schwarzenberg Complex and Losegg-Hofpürgl slice of the Lammer Unit can be explained by the burial and heat flow history of the Dachstein Nappe.

Acknowledgements

This study was financially supported by the Austrian Science Fund (FWF) due to grant P10277. R. Sachsenhofer provided us with unpublished vitrinite reflectance data. We thank M. Wagreich (Wien), R. Ondrak (Potsdam) and an anonymous reviewer for constructive criticisms.

References

Barker, C.E., 1988. Geothermics of petroleum systems: Implications of the stabilization of kerogen thermal maturation after a geologically brief heating duration at peak temperature. In: Magoon, L.B. (ed.), Petroleum system of the United States. U.S. Geological Survey Bulletin, 1870, pp. 26-29.

Colins, E., Hamilton, W. and Schmidt, F., 1992. The Hydrocarbon Potential of the Alpine Subthrust and Overthrust, Austria. In: Spencer, A.M. (ed.) Generation, Accumulation and Production of Europe's Hydrocarbons II. Special Publications European Association Petroleum Geosciences, 2, 193-199.

Ferreiro Mählmann, R., 1994. Zur Bestimmung von Diagenesehöhe und beginnender Metamorphose- Temperaturgeschichte und Tektogenese des Austroalpins und Südpenninikums in Vorarlberg und Mittelbünden. Frankfurter geowissenschaftliche Arbeiten, Serie C, 14, 1-498.

Ferreiro Mählmann, R. and Petschick, R., 1995. Illit-Kristallinität, Vitrinitreflexion und Maturitätsmodellierungen: Tektonische Fallstudien aus der Lechtal- und Silvretta Decke. In: Amann G., Handler R., Kurz W., Steyrer H.P. (eds.) 6. Symposium Tektonik-Strukturgeologie-Kristallingeologie, Erweiterte Kurzfassungen, Salzburg (Universität Salzburg) pp. 112-115.

Frisch, W. and Gawlick, H.-J., 2003. The nappe concept of the central Northern Calcareous Alps and its disintegration during Miocene tectonic extrusion – a contribution to understanding the orogenic evolution of the Eastern Alps. International Journal Earth Sciences, 92, 712-727.

Frisch, W., Kuhlemann, J., Dunkl, I. and Brügel, A., 1998. Palinspastic reconstruction and topographic evolution of the Eastern Alps during late Tertiary tectonic extrusion. Tectonophysics, 297, 1-15.

Frisch, W., Kuhlemann, J., Dunkl, I., Brügel, A. and Székely, B., 2001. The Dachstein paleosurface and the Augenstein Formation in the Northern Calcareous Alps - a mosaic stone in the geomorphological evolution of the Eastern Alps. International Journal Earth Sciences, 90, 500-518.

Gawlick, H.-J., 1996. Die früh-oberjurassischen Brekzien der Strubbergschichten im Lammertal – Analyse und tektonische Bedeutung (Nördliche Kalkalpen, Österreich). Mitteilungen der Gesellschaft Geologie Bergbaustudenten Österreich, 39/40, 119-186.

Gawlick, H.-J., 1997. Conodont Colour Alteration Idizes (CAI) - Eine Möglichkeit für die Kartierung des Öl- und Gasfensters in mehrphasig deformierten karbonatdominierten Sedimentbecken. Erdöl Erdgas Kohle, 113, 164-167.

Gawlick, H.-J. and Frisch, W., 2002. The Middle to Late Jurassic carbonate clastic radiolaritic flysch sediments in the Northern Calcareous Alps: sedimentology, basin evolution, and tectonics – an overview. Neues Jahrbuch Geologie Paläontologie Abhandlungen, 230, 163-213.

Gawlick, H.-J. and Höpfer, N., 1996. Die mittel- bis früh-oberjurassische Hochdruckmetamorphose der Hallstätter Kalke (Trias) der Pailwand - ein Schlüssel zum Verständnis der frühen Geschichte der Nördlichen Kalkalpen. Schriftenreihe Deutscher Geologischer Gesellschaft, 1, 30-32.

Gawlick, H-J. and Königshof, P., 1993. Diagenese, niedrig- und miteltemperierte Metamorphose in den südlichen Salzburger Kalkalpen - Paläotemperaturabschätzung auf der Grundlage von Conodont-Color-Alteration-Index-(CAI-) Daten. Jahrbuch der Geologischen Bundesanstalt, 136, 39-48.

Gawlick, H.-J., Leuschner, K. and Zankl, H., 1990. Neuinterpretation eines Querprofils durch die westliche Lammereinheit (Nördliche Kalkalpen, Österreich). Jahrbuch der Geologischen Bundesanstalt, 133, 561-566.

Gawlick, H.-J., Krystyn, L. and Lein, R., 1994. Conodont colour alteration indices: Paleotemperatures and metamorphism in the Northern Calcareous Alps - a general view. Geologische Rundschau, 83, 660-664.

Gawlick, H.-J., Frisch, W., Vecsei, A., Steiger, T. and Böhm, F., 1999. The change from rifting to drifting in the Northern Calcareous Alps as recorded in Jurassic sediments. Geologische Rundschau, 87, 644-657.

Haas, J., Kovács, S., Krystyn, L. and Lein, R., 1995. Significance of Late Permian-Triassic facies zones in terrane reconstruction in the Alpine-North Pannonian domain. Tectonophysics, 242, 19-40.

Hejl, E. and Grundmann, G., 1989. Apatit-Spaltspurendaten zur thermischen Geschichte der Nördlichen Kalkalpen, der Flysch- und Molassezone. Jahrbuch der Geologischen Bundesanstalt, 132, 191-212.

Kralik, M. and Schramm, M., 1994. Illit-Wachstum: Übergang Diagenese-Metamorphose in Karbonat- und Tongesteinen der Nördlichen Kalkalpen: Mineralogie und Isotopengeologie (Rb-Sr, K-Ar und C-O). Jahrbuch der Geologischen Bundesanstalt, 137, 105-137.

Kralik, M., Krumm, H. and Schramm, J.-M., 1987. Low grade and very low grade metamorphism in the Northern Calcareous Alps and in the Greywacke Zone: illite-crystallinity data and isotopic ages. In: H.W. Flügel and P. Faupl (eds.), Geodynamics of the Eastern Alps. Deuticke, Wien, pp. 164-178.

Krumm, H., Petschick, R. and Wolf, M., 1988. From diagenesis to anchimetamorphism, Upper Austroalpine sedimentary cover in Bavaria and Tyrol. Geodinamica Acta, 2, 33-47.

Kürmann, H., 1993. Zur Hochdiagenese und Anchimetamorphose in Permotrias-Sedimenten des Austroalpins westlich der Tauern. Bochumer geologische und geotechnische Arbeiten, 41, 1-328.

Linzer, H.G., Ratschbacher, L. and Frisch, W., 1995. Transpressional collision structures in the upper crust: the fold-thrust belt of the Northern Calcareous Alps. Tectonophysics, 242, 41-61.

Mandl, G.W., 2000. The Alpine sector of the Tethyan shelf – Examples of Triassic to Jurassic sedimentation and deformation from the Northern Calcareous Alps. Mitteilungen der Österreichischen Geologische Gesellschaft, 92, 61-77.

Neubauer, F., 1994. Kontinentkollision in den Ostalpen. Geowissenschaften, 12, 136-140.

Neubauer, F., Genser, J. and Handler, R., 2000. The Eastern Alps: Result of a two-stage collision process. Mitteilungen der Österreichischen Geologische Gesellschaft, 92, 117-134.

Petschick, R., 1989. Zur Wärmegeschichte im kalkalpin Bayerns und Nordtirols (Inkohlung und Illitkristallinität). Frankfurter geowissenschaftliche Arbeiten, Serie C, 10, 1-259.

Plöchinger, B., 1980. Die Nördlichen Kalkalpen. In: R. Oberhauser (ed.), Der geologische Aufbau Österreichs. Geologische Bundesanstalt, Wien, pp. 217-264.

Rantitsch, G., Melcher, F., Meisel, Th. and Rainer, Th., 2003. Rare earth, major and trace elements in Jurassic manganese shales of the Northern Calcareous Alps: Hydrothermal versus hydrogenous origin of stratiform manganese deposits of the Eastern Alps. Mineralogy and Petrology, 77, 109-127.

Sachsenhofer, R.F., 1987. Fazies und Inkohlung mesozoischer Kohlen der Alpen Ostösterreichs. Mitteilungen der Österreichischen Geologischen Gesellschaft, 80, 1-45.

Sachsenhofer, R.F., 2001. Syn- and post-collisional heat flow in the Tertiary Eastern Alps. International Journal Earth Sciences, 90, 579-592.

Schweigl, J. and Neubauer, F., 1997. Structural evolution of the central Northern Calcareous Alps: significance for the Jurassic to Tertiary geodynamics in the Alps. Eclogae Geologicae Helvetiae, 90, 303-323.

Spötl, Ch. and Hasenhüttl, Ch., 1998. Thermal history of the evapritic Haselgebirge mélange in the Northern Calcareous Alps (Austria). Geologische Rundschau, 87, 449-460.

Spötl, Ch., Kralik, M. and Kunk, M.J., 1996. Authigenic feldspar as an indicator of paleo-rock/water interactions in Permian carbonates of the Northern Calcareous Alps, Austria. Journal of Sedimentary Petrology, 66, 139-146.

Spötl, Ch., Kunk, M.J., Ramseyer, K. and Longstaffe, F.J., 1998. Authigenic potassium feldspar - a tracer for the timing of paleofluid flow in carbonate rocks, Northern Calcareous Alps, Austria. Geological Society of London Special Publication, 144, 107-128.

Sweeney, J.J. and Burnham, A.K., 1990. Evaluation of a simple model of vitrinite reflectance based on chemical kinetics. American Association Petroleum Geology Bulletin, 74,1559-1570.

Tollmann, A., 1976. Der Bau der Nördlichen Kalkalpen. Deuticke, Wien, 449 pp.

Wagreich, M., 1988. Sedimentologie und Beckenentwicklung des tieferen Abschnittes (Santon-Untercampan) der Gosauschichtgruppe von Gosau und Rußbach (Oberösterreich – Salzburg). Jahrbuch der Geologischen Bundesanstalt, 131, 663-685.

Wagreich, M., 1995. Subduction tectonic erosion and Late Cretaceous subsidence along the northern Austroalpine margin (Eastern Alps, Austria). Tectonophysics, 242: 63-78.

Wagreich, M., 2001. Paleocene – Eocene paleogeography of the Northern Calcareous Alps (Gosau Group, Austria). In: W.E. Piller and M.W. Rasser (eds.), Paleogene of the Eastern Alps. Österreichische Akademie der Wissenschaften, Schriftenreihe der Erdwissenschaftlichen Kommission, 14, pp. 57-75.

Wagreich, M. and Decker, K., 2001. Sedimentary tectonics and subsidence modelling of the type Upper Cretaceous Gosau basin (Northern Calcareous Alps, Austria). International Journal Earth Sciences, 90, 714-726.

Wagreich, M. and Faupl, P., 1994. Paleogeography and geodynamic evolution of the Gosau group of the Northern Calcareous Alps (Late Cretaceous, Eastern Alps, Austria). Palaeogeography, Palaeoclimatology, Palaeoecology, 110, 235-254.

Warr, L.N., Greiling, R.O. and Zachrisson, E., 1996. Thrust-related very low grade metamorphism in the marginal part of an orogenic wedge, Scandinavian Caledonides. Tectonics, 15, 1213-1229.

Received: 23. June 2005
Accepted: 23. November 2005

Gerd RANTITSCH[1] & Barbara RUSSEGGER[2]

[1] Department of Applied Geosciences and Geophysics, Montanuniversität Leoben, Austria, A-8700 Leoben, Austria,
Email: gerd.rantitsch@mu-leoben.at

[2] Library of the University of Graz, A-8010 Graz, Austria